Snap-back induced hysteresis in an elastic mechanical metamaterial under tension

Cite as: Appl. Phys. Lett. **115**, 091901 (2019); https://doi.org/10.1063/1.5119275
Submitted: 11 July 2019 . Accepted: 13 August 2019 . Published Online: 26 August 2019

Shanwen Sun, Ning An, Guoli Wang, Meie Li, and Jinxiong Zhou

Applied Physics Letters ARTICLE scitation.org/journal/apl

Snap-back induced hysteresis in an elastic mechanical metamaterial under tension

Cite as: Appl. Phys. Lett. **115**, 091901 (2019); doi: 10.1063/1.5119275
Submitted: 11 July 2019 · Accepted: 13 August 2019 ·
Published Online: 26 August 2019

Shanwen Sun,[1] Ning An,[1] Guoli Wang,[1] Meie Li,[2,a)] and Jinxiong Zhou[1]

AFFILIATIONS

[1]State Key Laboratory for Strength and Vibration of Mechanical Structures, Shaanxi Engineering Laboratory for Vibration Control of Aerospace Structures, School of Aerospace, Xi'an Jiaotong University, Xi'an 710049, China
[2]State Key Laboratory for Mechanical Behavior of Materials, School of Materials Science and Engineering, Xi'an Jiaotong University, Xi'an 710049, China

[a)]Author to whom correspondence should be addressed: limeie@mail.xjtu.edu.cn

ABSTRACT

We combine experiment and finite element simulation and come up with a design for a mechanical metamaterial which demonstrates snap-back induced hysteresis and energy dissipation. The resultant is an elastic system that can be used reversibly for many times. The underlying mechanism of the existence of hysteresis and the physics of snap-back induced elastic instability is unveiled. Our results open an avenue for the design and implementation of recoverable energy dissipation devices by harnessing mechanical instability.

Mechanical hysteresis, characterized by noncoincident loading-unloading curves, is a ubiquitous phenomenon in many dissipative or rate-dependent systems such as viscoelastic and elastoplastic systems or systems where a phase transition occurs such as shape memory alloys.[1] In general, an otherwise elastic system does not dissipate energy and exhibits hysteresis undergoing a loading-unloading cycle. Hysteresis, nevertheless, can be achieved in elastic systems by leveraging mechanical instability mainly through compression, opening the door for multistable mechanical metamaterials for various applications.[2–12] In a system undergoing instability, the force-displacement curve is not monotonic. Snap-through instability occurs when the displacement jumps suddenly in a load-control case. A counterpart, the so-called snap-back instability, occurs in a displacement-control system when load jumps suddenly even without an increase in the prescribed displacement.[13] Recently, a mechanical metamaterial sheet had a regular pattern of holes with two different sizes and confined deformation along one axis by compressing the sheet along the direction perpendicular to the confinement axis. Snap-back instability and hysteresis are achieved in a displacement-control way.[14] However, the introduction of confinement complicates the implementation and entails the instability confinement-dependent.

An intriguing yet elusive question is that can snap-back instability be realized in a tensile loading case? Here, we explore the snap-back instability induced hysteresis in a mechanical metamaterial without confinement and under a tensile loading case. Snap-through instability was observed in a similar mechanical metamaterial under tensile load-control way.[15] But as we explain later, such a system does not exhibit snap-back instability and hysteresis in a displacement-control scheme. From an experimental viewpoint, displacement-control is more favorable and more straightforward to realize.

We start with the numerical simulation of a mechanical metamaterial sheet with periodic patterns. Due to periodicity, we only need to model a representative volume element (RVE) and apply periodic boundary conditions (supplementary material). Figure 1(a) shows the RVE of the mechanical metamaterial sheet which is stretched vertically at two edges. Periodic boundary conditions were enforced on the upper and lower horizontal and left and right vertical sides. The RVE consists of two centrally connected cosine-shaped slender segments, one is slim and the other is fat in thickness, which can be tessellated in plane to form a periodic arrangement. This was previously studied by Rafsanjani *et al.*[15] but only the loading curve was given. The RVE was chosen here to serve as an example to elucidate the difference between displacement- and load-control loadings (supplementary material). Figure 1(b) shows the deformation contours of the RVE at various applied displacements. Figure 1(b) indicates that the upper slim beam undergoes shape transformation at various applied stretches, changing the curvature from convex to concave, while the lower fat beam deforms a little bit but remains unchanged in shape. Figure 1(c) plots the normalized nominal stress vs strain curve. The nominal stress is obtained from the reaction force divided by the reference cross

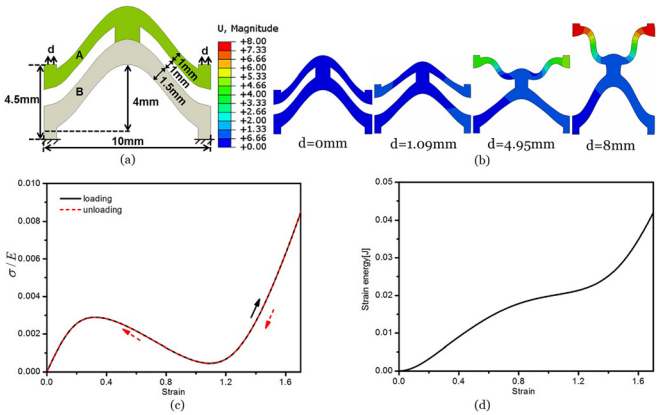

FIG. 1. RVE and deformation of a mechanical metamaterial with zero hysteresis under tension. (a) RVE dimensions and boundary conditions of an RVE under tension of a mechanical metamaterial sheet. (b) Deformation contours of the RVE. (c) The normalized stress-strain curve of the RVE undergoes a displacement-controlled loading-unloading process. (d) The strain energy vs applied strain.

sectional area and then normalized by the modulus of the material E (5.01 MPa). The strain is calculated by dividing the vertical displacement by the height of the RVE [4.5 mm in Fig. 1(a)]. For a force-control case, load is prescribed and increased monotonically; for a displacement-control case, displacement is prescribed and the force is extracted as a reaction from simulation. Figure 1(c) shows that the force and the resultant stress first increase as the applied strain increases and then peaks out, where the upper beam changes the curvature; the stress then decreases as the prescribed strain increases further as the upper beam changes curvature and eventually goes up when the RVE is stretched most, but there is no instability in such a displacement-control scenario. This N-shaped force-displacement curve can be understood as follows. The upper cosine-shaped slim segment can be regarded as two inclined cantilevered beams. Subjected to the vertical prescribed displacement constraints, the two inclined beams are bent and compressed. The compression in the inclined beam first increases as the applied displacement increases, but the following shape transition of the inclined beams causes part of the compression to relax, giving the up and down trend of the force-displacement curve. In Fig. 1(c), the black solid line is the loading path, while the red dashed line is the unloading path. The loading and unloading curves coincide with each other in such a displacement-control way. In the supplementary material, we give both loading and unloading curves and seriously compare the load-control and displacement-control cases. The unloading curve is missing in the previous study;[15] thus, it is impossible to estimate hysteresis loop and energy dissipation. Figure 1(d) plots the strain energy vs applied displacement curve during the loading process. Note that as the applied displacement increases monotonically, so does the stored strain energy in the system. The RVE in Fig. 1(a) does not exhibit hysteresis in a displacement-control way, but hysteresis exists if the same system is loaded in a forced-control way (supplementary material). For the RVE in Fig. 1(a) and that studied in Ref. 15, the external work was converted into the form of strain energy and stored mainly in the inclined beam A and partially in beam B. Subjected to a displacement-control loading-unloading cycle, the bending and relaxing of beam A is a stable deformation process and the stored strain energy curve is monotonic as indicated in Fig. 1(d). Thus, no snap-back instability occurs in the RVE in Fig. 1(a) and that in Ref.15.

We present in Fig. 2(a) the RVE of another mechanical metamaterial. It comprises two unit cells in Fig. 1(a) in series. But this simple combination yields mechanical behavior quite different from that in Fig. 1. The RVE of the design consists of four curved segments, marked by A, B, C, and D, respectively. A and C are slim beams, and B and D are thick ones. Compared with beams A and D, beams B and C are shorter in length. Figure 2(b) shows the snapshots of deformation contours corresponding to various applied displacements. When applied displacement d = 5.47 mm, the slim beam C with a shorter length has already completed curvature reversing, while beam A with a longer length remains curvature unchanged but in the vicinity of curvature transition. Fat beams, B and D, deform but remain shape unchanged. If the applied displacement increases beyond a critical value, say d = 5.58 mm, beam A snaps and undergoes curvature reverse, too. The snap and curvature reverse of beam A results in a downward displacement in the midpoint of beam A, and this downward displacement propagates through beam B and pushes beam C back to its original configuration. The existence and the snapping-back of beam C are crucial for the instability of the design, which shows the force-displacement in Fig. 2(c). At d = 5.58 mm, a sudden drop occurs in the force-displacement curve, as indicated by the arrow. As the applied displacement is increased to a high value, say d = 12 mm, beam C reverses the curvature for the second time. If one reverses the process, the unloading path is given by the red dashed line. Clearly, the unloading curve does not coincide with the loading curve, and there exists a hysteresis marked by the shaded area in Fig. 2(c). Figure 2(d) plots the strain energy-displacement curve, and it is not monotonic, and a drop occurs when beam C snaps back. Snapping back releases part of the stored strain energy which is converted into kinetic energy and dissipated eventually (supplementary material).

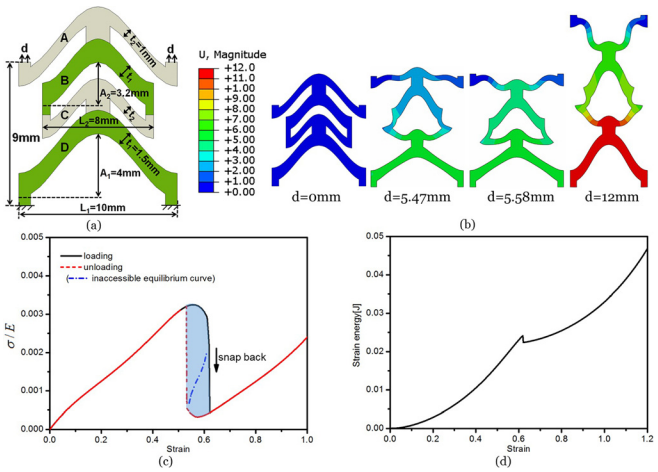

FIG. 2. RVE and deformation of a mechanical metamaterial under tension exhibiting hysteresis and energy dissipation. (a) RVE dimensions and boundary conditions of the RVE of the metamaterial design. (b) Deformation contours of the RVE for various applied stretches. (c) The loading-unloading curve of the RVE under a displacement-control manner. The snapping back and the dissipated energy are marked for eye view. (d) The strain energy vs strain curve.

It is more informative, and the underlying physics is unveiled comparing Figs. 1(c) and 1(d) with Figs. 2(c) and 2(d). In Fig. 1(c), all the loading and unloading paths are physically accessible and a collection of infinitesimal neighborhoods of configurations in the displacement-control experiment. This is not the case in Fig. 2(c), and there exists an inaccessible equilibrium path given by the blue dash dot line in the hysteresis loop. The configurations are not infinitesimal neighborhoods, and jump phenomenon occurs when snapping back occurs.

Our design in Fig. 2(a) has several geometric design parameters. The above-mentioned discussion is related to a set of typical geometric parameters: $t_1 = 1.5$ mm, $t_2 = 1$ mm, $A_1 = 4$ mm, $A_2 = 3.2$ mm, $L_1 = 10$ mm, and $L_2 = 8$ mm. Definitely, these parameters can be varied to check various designs. We performed detailed parametric analysis and performed nearly 1000 finite element simulations (supplementary material) and finally identified that the ratio of t1/t2 and the normalized height of A1/L1 are two key parameters to control the snap-back behavior of the metamaterial. Actually, these two parameters characterize the slimness of the beam and the inclination of the convex arch, which are more sensitive to the snap-back instability of the RVE. We then carried out a series of finite element calculations (supplementary material) and constructed the phase diagram in terms of A1/L1 and t1/t2 in Fig. 3. The gray area is the space without snap-back, and the snap-back region is marked by different colors, corresponding to different dissipated energy due to hysteresis and indicated by the scale bar.

To further prove the previous analysis based on RVE, we fabricated finite size structures consisting of 13×2 RVEs and performed experiment and simulation, highlighting the difference of two RVEs. The results are presented in Figs. 4 and 5, corresponding to RVE without and with snap-back, respectively. The sample was fabricated via a reverse mold (fabrication precision 0.2 mm) and was made of polyurethane rubber. The sample was loaded in a quasistatic way with a loading rate of 0.5 mm/s (displacement precision 0.0001 mm, force precision 0.0001 N). In the nominal stress-strain curves in Fig. 4, the black solid line is the loading path, and the blue dashed line is the unloading path in the experiment. The red solid line and green dashed line are the simulations for loading and unloading paths, respectively. Note that the polyurethane rubber is viscoelastic; so, there exists a hysteresis in the experiment. Simulation here adopts the Neo-Hookean hyperelastic model (G = 1.67 MPa, $\mu = 0.49$), and the unloading curve

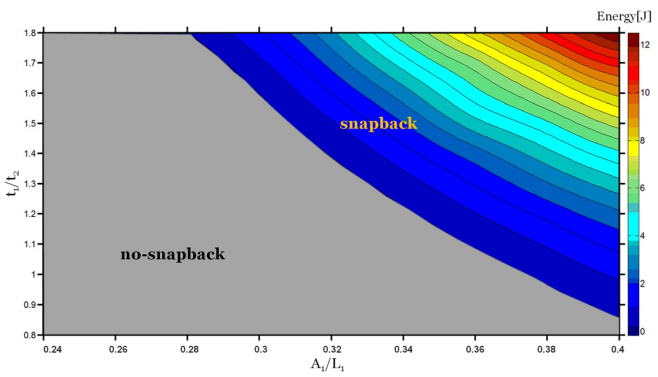

FIG. 3. The instability phase diagram of the RVE in Fig. 2 and the associated dissipated energy.

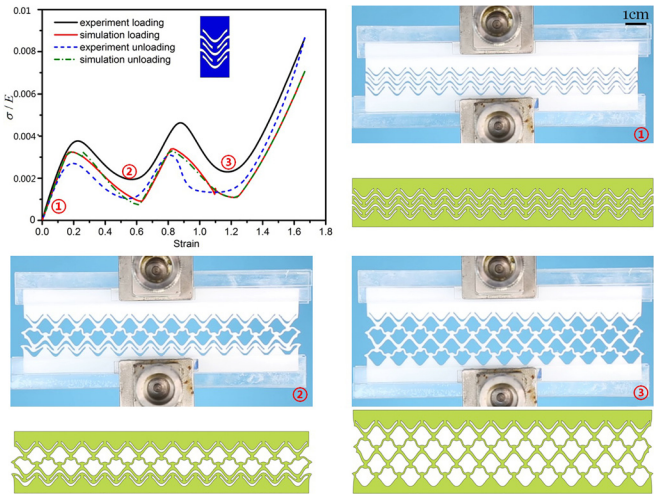

FIG. 4. Loading-unloading behavior of a mechanical metamaterial sheet with 13×2 RVEs given in Fig. 1. Both snapshots of experiment and simulation are given for comparison. Instants ①, ②, and ③ are marked in the stress-strain curve.

almost coincides with the loading curve with zero hysteresis. In Fig. 4, snapshots of experiment and simulation are given for comparison, and good agreement is achieved albeit of the discrepancy due to the material model. Both experiment and simulation reveal the sequential

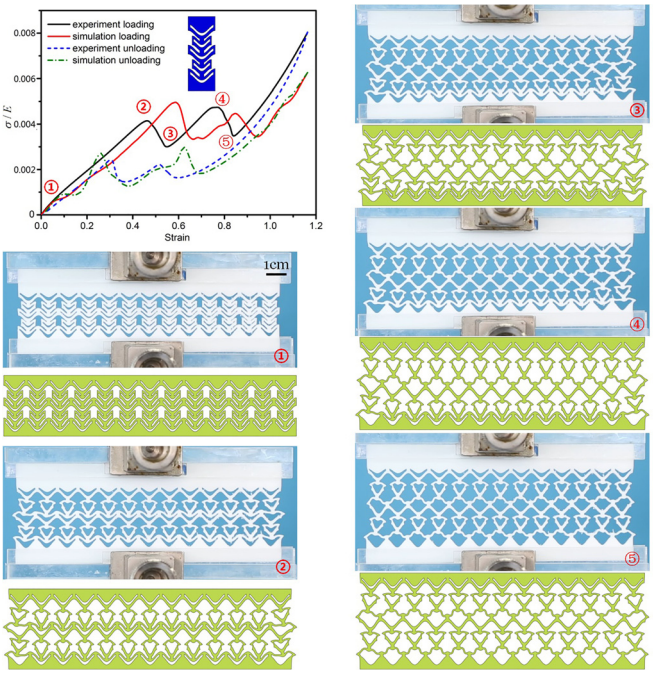

FIG. 5. Deformation and snap-back induced hysteresis of a mechanical metamaterial with 13×2 RVEs given in Fig. 2. Both snapshots of experiment and simulation are given for comparison. Instants ①, ②,④, and ③⑤ are marked in the stress-strain curve.

curvature reversing process, reflected in the wavy profile of the stress-strain curve. The instant marked by ① is the original state; state ② is one of the local extrema in the stress-strain curve, where the top layer of slim beams completes curvature reversing, as shown in the snapshots; state ③ is another local extremum where the top and bottom layers of slim beams undergo shape transition (see Movie_S1).

Figure 5 plots the nominal stress-strain curve of the finite structure derived from the RVE exhibiting hysteresis from simulation by using the same hyperelastic material parameters previously mentioned. A marked difference is that the structure in Fig. 5 does exhibit hysteresis, dissipating about 0.128 J energy by evaluating the enclosed area of the hysteresis. Experimentally, the loading-unloading process dissipates about 0.143 J energy, a little bit larger than that predicted by simulation due to the fact that the overall dissipated energy in experiment includes the part due to material viscoelasticity and the part due to snap-back instability, whereas the material viscoelasticity is not accounted for in simulation. Both experiments and simulations reveal that the system undergoes a similar sequential curvature reversing. Slender beam C with shorter length reverses first in a layer by layer fashion. After beam C completes its curvature reversing, then beam A begins to reverse if applied displacement is further increased. Snap-back of beam C occurs in the stages of ③ and ⑤, as shown in the figure (see Movie_S2).

In summary, we come up with an elastic mechanical metamaterial which exhibits a snap-back induced hysteresis under tension. Upon loading and unloading, the elastic system dissipates the amount of energy due to hysteresis loop. The deformation and the dissipation processes are reversible, and the system can be used in a rate-independent manner for many cycles, opening an avenue for reversible energy dissipation through mechanical instability.

See the supplementary material for the details of numerical simulations and movies recorded in experiments.

This research is supported by the Natural Science Foundation of China (Grant Nos. 11472210 and 11372239) and by a technological project of Institute of Systems Engineering, China Academy of Engineering Physics (No. 2017KJZ06).

REFERENCES

[1]G. Bertotti and I. D. Mayergoyz, *The Science of Hysteresis: Hysteresis in Materials* (Gulf Professional, 2006), Vol. 3.
[2]D. M. Correa, T. Klatt, S. Cortes, M. Haberman, D. Kovar, and C. Seepersad, Rapid Prototyping J. **21**, 193 (2015).
[3]S. Shan, S. H. Kang, J. R. Raney, P. Wang, L. Fang, F. Candido, J. A. Lewis, and K. Bertoldi, Adv. Mater. **27**, 29 (2015).
[4]K. Bertoldi, Ann. Rev. Mater. Res. **47**, 51 (2017).
[5]D. M. Kochmann and K. Bertoldi, Appl. Mech. Rev. **69**, 5 (2017).
[6]C. S. Ha, R. S. Lakes, and M. E. Plesha, Mater. Des. **141**, 426 (2018).
[7]B. Haghpanah, L. Salari-Sharif, P. Pourrajab, J. Hopkins, and L. Valdevit, Adv. Mater. **28**, 36 (2016).
[8]T. Frenzel, C. Findeisen, M. Kadic, P. Gumbsch, and M. Wegener, Adv. Mater. **28**, 5865 (2016).
[9]C. Findeisen, J. Hohe, M. Kadic, and P. Gumbsch, J. Mech. Phys. Solids **102**, 151 (2017).
[10]K. Bertoldi, V. Vitelli, J. Christensen, and M. van Hecke, Nat. Rev. Mater. **2**, 11 (2017).
[11]J. Meaud and K. Che, Int. J. Solids Struct. **122**, 69 (2017).
[12]H. Yang and L. Ma, Mater. Des. **152**, 181 (2018).
[13]R. M. Jones, *Buckling of Bars, Plates, and Shells* (Bull Ridge Corporation, 2006).
[14]B. Florijn, C. Coulais, and M. van Hecke, Phys. Rev. Lett. **113**, 17 (2014).
[15]A. Rafsanjani, A. Akbarzadeh, and D. Pasini, Adv. Mater. **27**, 5931 (2015).

Supplementary material

Title: Snap-back induced hysteresis in an elastic mechanical metamaterial under tension

S1: RVE simulation details and difference between displacement- and force-control

We choose here the RVE shown in FIG.1(a) as a typical example to detail the simulation details. The RVE was stretched vertically at two upper edges, while the vertical displacements of the bottom edges were constrained. Periodic boundary conditions were enforced on the upper and lower horizontal and left and right vertical sides. The geometric modeling of the RVE was performed in a parametric way by Python script, which facilitates parametric study described in the following. For the polymeric sheet considered here, a nearly incompressible hyperelastic Neo-Hookean material model was adopted with shear modulus 1.67 MPa and Poisson's ratio 0.49. The deformation of the RVE sheet was treated as a plane stress problem and the RVE was discretized by 6-node quadratic triangle elements (CPS6). All simulation were carried out in ABAQUS 6.14. The RVE was modeled either in a displacement-control or in a force-control way, and various algorithms provided in ABAQUS were used.

For a structure which is loaded in a quasi-static loading, the deformation of the

structure can be captured either by static/general or dynamic/implicit algorithms. In this study, both were utilized and both can give identical solutions. But for most cases, the dynamic algorithm has better convergence than the static/general algorithm. We model all the displacement-control cases by using dynamic/implicit, while all force-control cases are modeled by using static/general. Specific choice of algorithms does not affect the results, and each case can be reproduced by proper usage of algorithms.

FIG.S1 plots the force-displacement curve of the RVE in FIG.1(a). Both loading and unloading curves are presented and indicated by the arrows. The black solid line and the red dashed line represent the loading and unloading curves in the displacement-control way. The blue filled triangle and the purple filled inverted triangle denote the loading and unloading curves in the force-control way. FIG.S1 clearly shows the difference between displacement- and force-control loading processes. The loading curve coincides with the unloading curve in the displacement-control case, and there is no jumps and hysteresis for the RVE in FIG.1(a). All the loading and unloading paths are in equilibrium states and are physically accessible. In the force-control case however, the RVE in FIG.1(a) undergoes snap-through instability and there is hysteresis in a loading-unloading cycle. When the applied load reaches a critical value, jump of displacement occurs even without increase of loading, resulting in the snap-through instability. The critical conditions for the onset of snap-through instability are not the same in the loading and the unloading processes, thereby forming hysteresis.

Similar simulations were performed regarding the RVE in FIG.2(a), which gives the results plotted in FIG.S2. The force-control process is denoted by black filled square, and the displacement-control process is represented by red filled circle. The loading and unloading paths are indicated by arrows. Note that similar snap-through instability occurs in the force-control process as expected. The marked difference between FIG.S1 and FIG.S2 is that there does exist instability in the displacement-control case in FIG.S2. As explained in the main text, the force-displacement curve in FIG.S2 undergoes snap-through instability in load-control case; meanwhile, it also exhibits so-called snap-back instability in displacement-control case. In contrast, the force-displacement curve in FIG.S1 only exhibits snap-through instability in force-control case and there is no instability in displacement-control case. Also note that there is a branch of inaccessible equilibrium path as marked by blue dotted line, and this branch is captured by using the static/Riks algorithm. FIG.S3 plots the associated energy versus displacement curve for the RVE in FIG.2(a). The black line is the external work, the red line is the strain energy, and the blue line is the kinetic energy. The kinetic energy remains nearly zero during the whole loading process except a small increase presented in a zoomed in picture inserted in FIG.S3. The occurrence of the increase of kinetic energy corresponds to a drop in the strain energy. The drop of the strain energy is converted into the increase of the kinetic energy. The sum of strain energy and the kinetic energy always equals to the work done by external force, a statement of energy conversation as expected.

S2: Construction of instability phase diagram

To construct an instability diagram and to explore the influence of various geometric parameters on the snap-back instability, the finite element model of the RVE in FIG.2(a) is needed to be built by parametric modeling via a Python script. Various geometric parameters defining the geometry of the RVE are defined as variables rather than fixed values. A MATLAB code was written to execute the running of ABAQUS. All together, nearly 1000 finite element simulations were carried out. For each group of parameters, the force-displacement curves for both loading and unloading processes were obtained, and a MATLAB code was used to calculate the enclosed area giving the energy dissipation during a complete cycle. The calculated energy dissipation was stored a series of arrays, and a function in MATLAB, contourf, was used to plot the phase diagram shown in FIG.S4 and FIG.3.

S3: Material characterization and experiment

FIG.S5(a) shows the standard material sample which was used to measure material constants. FIG.S5(b) plots the obtained experimental stress-strain curve of the sample. The material used in sample fabrication is polyurethane rubber and a finite size structure consisting of 13×2 RVEs was fabricated by reverse mould and was shown in FIG.S5(c).

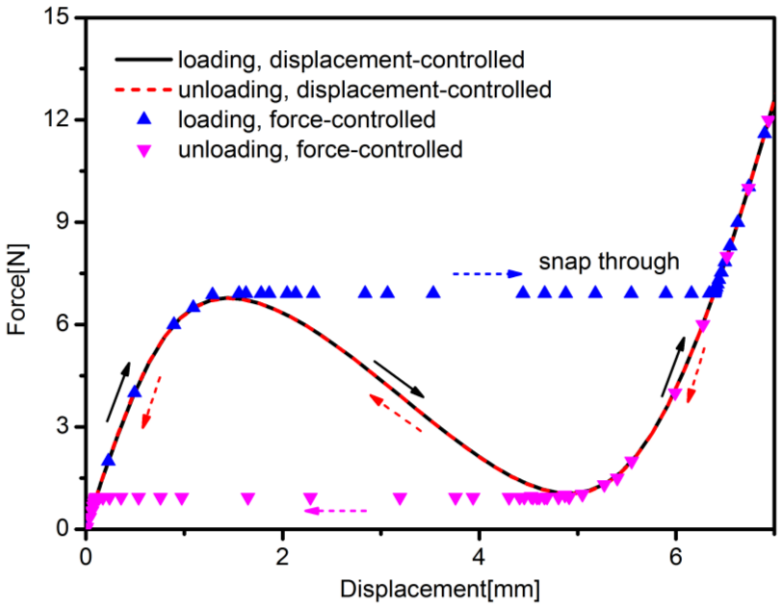

FIG.S1 The force-displacement curve of the RVE in FIG.1(a) in the displacement- and force-way

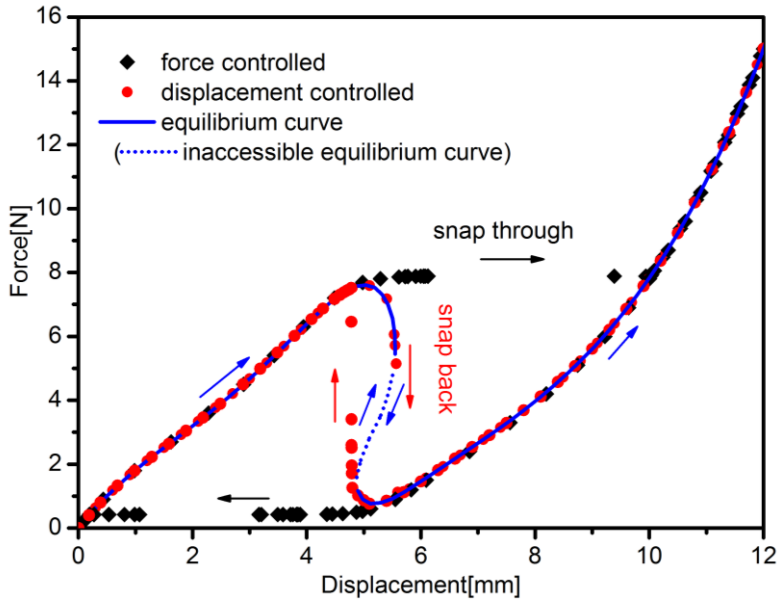

FIG.S2 The force-displacement curve of the RVE in FIG.2(a) in the displacement- and force-way

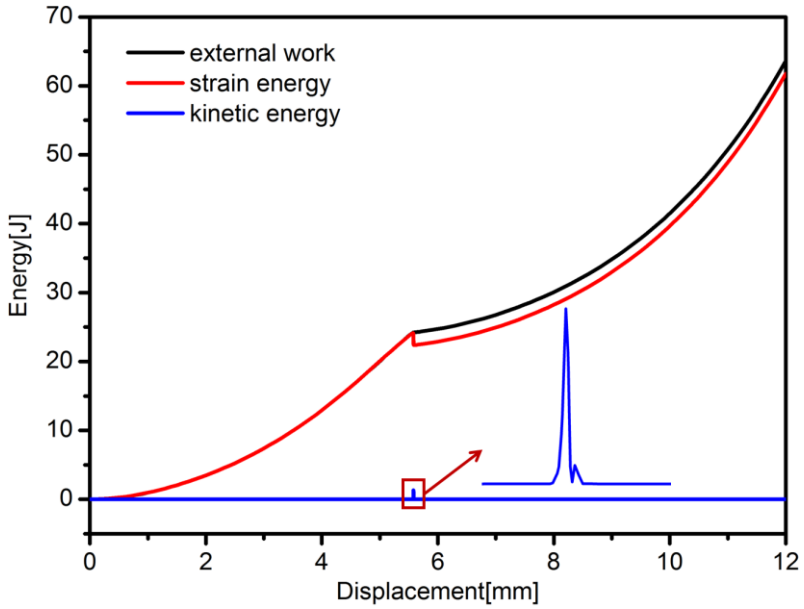

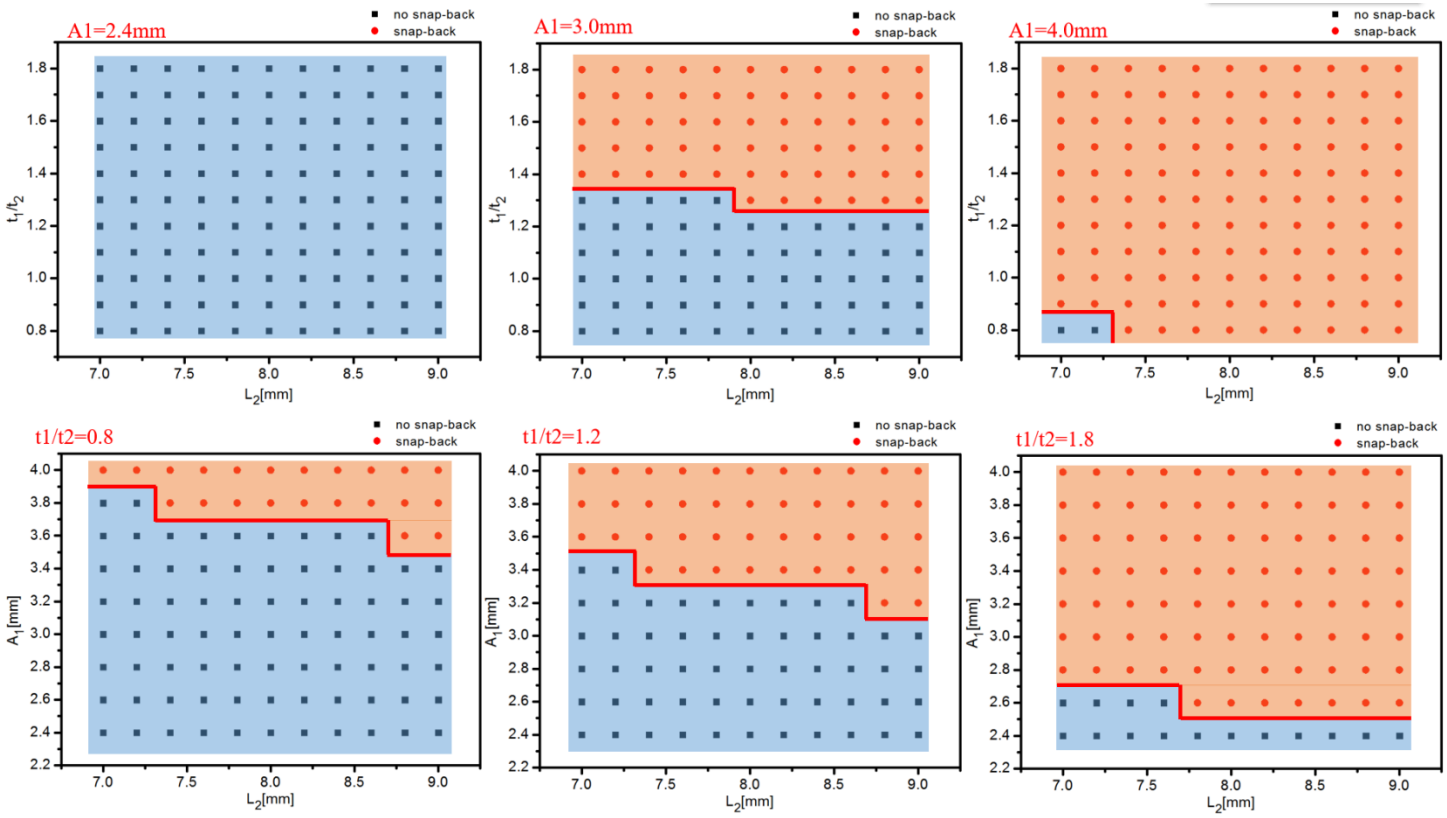

FIG.S3 The associated energy versus displacement curve for the RVE in FIG.2(a)

FIG.S4 The influence of various geometric parameters on the snap-back instability

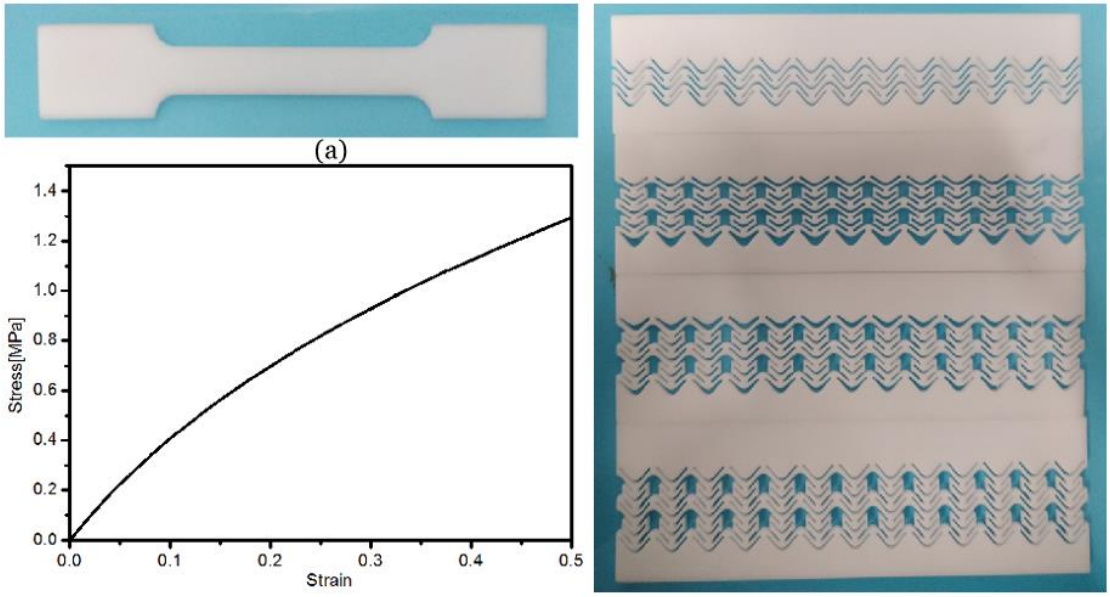

FIG.S5 Material Characterization and experiment strucure